

Detectability of flat microdefects in radiographic images obtained using linear microfocus bremsstrahlung source based on 18 MeV betatron with narrow target inside

M M Rychkov, V V Kaplin and V A Smolyanskii

National Research Tomsk Polytechnic University, Tomsk, Russia

rychkov@tpu.ru

Abstract. For the determination of ability of microfocus Bremsstrahlung (Bs) source based on B-18 betatron to detect flat microgaps and microinclusions in heavy material products the investigations were carried out. The radiographic images of 10 μm gaps and 13 μm tantalum (Ta) foil into steel bulk which were oriented at different angles with respect to the direction of radiation were investigated. The assembly of four steel blocks having 10 μm gaps between their neighbor surfaces was placed on goniometer. The 13 μm Ta foil having the length of 4 mm along radiation beam was mounted in a plastic holder which was also placed on the goniometer. For modeling narrow gaps and thin inclusions inside the bulk of steel detail, the experimental samples were placed before a thick steel plate. The radiographic images of the samples were obtained with a 2.4-fold magnification at different orientations of narrow gaps and Ta foil with respect to the radiation beam and at the thick steel plates of different thicknesses. The results illustrate high sensitivity of detecting of the microgaps inside steel bulk and flat microinclusions from heavy material in the bulk of detail made from a lighter material due to the microfocus of Bs source.

1. Introduction

The production of a microfocus radiation source based on relativistic electron beams is an important part of accelerator physics. The betatrons generating secondary hard radiation caused by interaction of the internal electron beam with the target (typically a thick target) that is larger in its area than the cross section of the millimeter-sized beam are used for obtaining the images of a number of objects. But, it is shown in [1] that the linear microfocus Bremsstrahlung (Bs) source can be created on the base of the 18-MeV betatron with internal thin flat target oriented along the electron beam. For the first time the idea of the use of the internal targets with a much smaller diameter than that of the internal electron beam of cyclic accelerators in order to reduce the focal spot of the generated radiation was proposed in [2]. Here, if the electron beam circulates during a sufficiently long time on the radius of the microtarget location, then, due to betatron oscillations, the electrons will fall on such a target with a sufficiently high efficiency. Later, this effect was realized on a miniature synchrotron [3].

Magnified images of the standard microstructure of the device Duplex IQI were obtained using the radiations generated in three narrow internal 50 and 8 μm Si and 13 μm tantalum (Ta) targets of the 18 MeV betatron. The width of the thinnest target was approximately 190 times smaller than the diameter (about 1.5 mm) of the electron beam. The formation of the device Duplex IQI [4] images with participation of the absorption and edge refraction contrast was shown. Good resolution of the pairs of



thinnest (50 μm) Pt wires of the microstructure of the device Duplex IQI was shown. It was shown also that the image contrast depends on the position of the microstructure in the radiation cone.

This work is devoted to the study of an ability of a microfocus source created on the base of the 18-MeV betatron to detect the flat internal microdefects of heavy material products. The result of the radiographic investigations which show the ability of new microfocus source to detect the micro-gaps and flat heavy inclusions with micro-thicknesses in heavy material products are presented. Images of the objects of research were obtained with a magnification of 2.4 using hard Bremsstrahlung ($E_\gamma > 1$ MeV) generated in a 13 μm Ta foil-target oriented along the electron beam using a goniometer inside the betatron chamber.

The magnified images of an assembly of four steel parallelepipeds, which are composed with the 10 μm gaps between them are presented. The magnified images of a Ta foil 13 μm thick and a length of 4 mm along the beam of microfocus radiation are also shown. To simulate the gaps and flat Ta inclusion in the steel bulk, the assembly of steel parallelepipeds and Ta foil in the holder were placed before a thick steel plate.

The presented results demonstrate high detectability of flat extended micro-inclusions made of heavy material in the thickness of the products made of lighter material and micro-gaps between the surfaces of joined parts of composite products due to the microfocus of the radiation source based on the 18 MeV betatron.

2. Experimental setup

The scheme of the experiment is shown in Figure 1. In a betatron B-18, a special system for reducing the orbit radius after electron acceleration provided a long-term discharge of the circulating electron beam, (1) in Figure 1a, on a narrow target (2) oriented along the electron beam using an internal goniometer (3). A tantalum foil 13 μm thick and 4 mm long along the electron beam was used as narrow target. The generated radiation with photon energies up to the energy of 18 MeV came out through the window of the experimental chamber, closed by 50 μm Mylar film, then passed through the experimental sample (4), installed in the external goniometer at a distance of 48 cm from the target, and a thick steel plate-absorber (5), and fell on the X-ray film (6) installed at a distance of 114 cm from the target. The external goniometer made it possible to orient the sample in the cone of radiation. The plate (5) was used to absorb the soft part ($E_\gamma < 1$ MeV) of Bremsstrahlung and also for the simulation of disposition of the gap defects or heavy inclusions inside the steel bulk.

The first sample is an assembly of rectangular steel parallelepipeds with dimensions of $9 \times 10 \times 30$ mm³, (1) in Figure 1b, connected to 10 μm gaps between them. The second test sample contains the Ta foil, (1) in Figure 1c, in a holder consisting of two plastic blocks in an external goniometer, which allowed the sample to be oriented in the radiation cone.

The obtained radiographic images of the samples were processed with a scanner for their analysis and obtaining densitograms of the images.

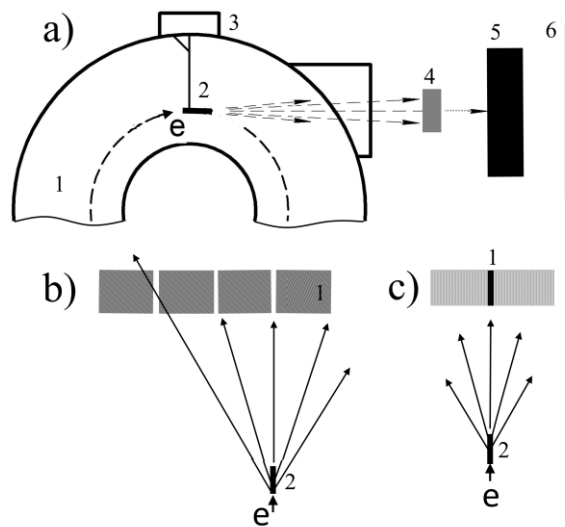


Figure 1. The experimental scheme: a) 1 – betatron chamber, 2 – Ta target, 3 – goniometer, 4 – object for radiography, 5 – thick steel plate, 6 – X-ray film; b) Location of four-steel-blocks assembly with three gaps on radiation beam emitted from 13 μm Ta target oriented along electron beam; c) Location of 13 μm Ta foil (mounted inside plastic holder) on radiation beam emitted from 13 μm Ta target.

3. Experiment with the gaps object

Figure 2 shows the photo of the angular distribution of radiation generated by electrons with an energy of 18 MeV in 13 μm Ta foil oriented at an angle $\theta_0 = 0^\circ$ relative to the electron beam. The photo of the radiation beam is formed by hard radiation, since the soft radiation is suppressed by absorption in the Ta target. This is evidenced by the presence of an image of the thick output flange of the betatron chamber window, which is not observed in the photos obtained in [1] using softer photons generated in 50 μm Si plate.

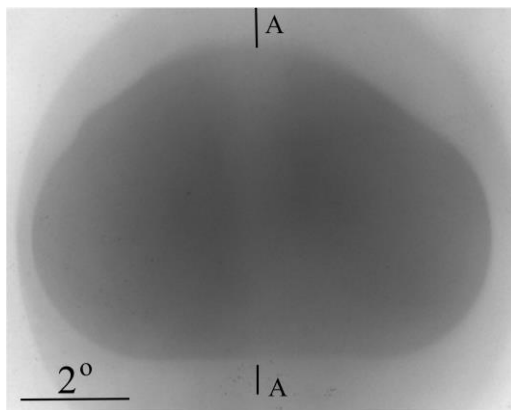


Figure 2. Photographs of angular distribution of Bs generated at 13 μm Ta target orientation $\theta_0 = 0^\circ$ with respect to the direction of electron beam. Vertical A–A shows target-plane projection crossing through radiation cone axis.

Figure 3 shows images of an assembly of four steel blocks with 10 μm gaps between them, which were obtained with a magnification of 2.4 using hard Bremsstrahlung generated in the 13 μm Ta target oriented along the electron beam. The image demonstrates a good resolution of the gaps in the sample. In this case, the radiation emitted along the direction of the plane of the Ta target, has a linear focus with a width of 13 μm and a height equal to the diameter of the electron beam (1.4 mm). The image (2a) of the assembly was obtained by orienting the right gap along the vertical line A–A (see, Figure 2) passing through the axis of the radiation cone. The angle between the gap walls and the radiation beam axis $\theta_g = 0^\circ$ (see, Figure 1b). The width of the image of this gap is less than the widths of the middle and left gaps. This is clearly seen in Figure 3b, which presents the gap images increased additionally. The width of the gap images increases from the gap to the gap (from right to left), and the contrast of the gap images decreases. The broadening of the images of the middle and left gaps is determined by their displacement l_g with respect to the axis of the radiation cone. This leads to an

increase in the angle θ_z of the orientation of the blocks surfaces forming the gaps relative to the axis of the radiation cone and also due to an increase of its projection $l_g \cdot \theta_z$. The width S_g of the gap image can be estimated as $S_g = L_2(((t_g + l \cdot \theta_g) + S_e) / L_1) - S_e$, where t_g and l are the width and length of the gap, L_1 and L_2 are the distances from the target to the sample and to the X-ray film, S_e is the effective horizontal size of the radiation source, which is $S_e = t_g + T \cdot \theta_g$, where $t = 13 \mu\text{m}$ is the thickness of the target, $T = 4 \text{ mm}$ is its length along the electron beam, $\theta_g = l_g / L_1$ – horizontal angle of emission of radiation from the target in the direction to the gap. It is seen that S_g increases with increasing angle θ_g .

Figure 3(c) shows the images of the right and middle gaps at the thickness of the steel plate-absorber placed behind the foil in the holder of 20 and 40 mm, left and right images, respectively.



Figure 3. Images of the sample with $10 \mu\text{m}$ gaps between the steel blocks: a) the image obtained with magnification of 2.4; b) additional enlarged images of the left, middle and right gaps of the steel sample; c) images of the middle and right gaps in the upper part of the steel sample obtained with an additional steel plate-absorber with thickness of 20 (left) and 40 mm (right), respectively.

Arrows show the edges of images of a steel plate 0.5 mm thick placed just after assembly.

As the thickness of the plate increases, the contrast of the slit image decreases, as more and more hard radiation forms the image of the foil, due to the absorption of the soft part of the spectrum of the generated radiation in the plate-absorber. However, it can be seen that the presence of gaps in the assembly is confidently detected in both cases.

4. Experiment with the Ta foil

Figure 4 shows the 2.4-magnified images of Ta foil, which is oriented at an angle $\theta_f = 0.6^\circ$ relative to the axis of the radiation cone (a) and along the axis of the radiation cone $\theta_f = 0^\circ$ (b). One can clearly see the foil image (light vertical strip), which becomes narrower with decreasing angle θ_f . The length of the foil along the radiation beam is 4 mm, which provides a strong absorption of hard radiation and forms a clear image of the foil due to the absorption contrast. Some contribution to the formation of contrast can also make the phase contrast [5] at $\theta_f = 0^\circ$. Figure 4 show the Ta foil images at the thickness of the steel plate placed behind the Ta foil (see Figure 1a), 20 (c) and 55 (d) mm. As the thickness of the plate increases, the contrast of the Ta foil image decreases because harder radiation forms the foil image, due to the absorption of the soft part of the generated radiation spectrum in the

steel plate. However, it can be seen that the presence of Ta foil behind the 55 mm steel plate is confidently determined.

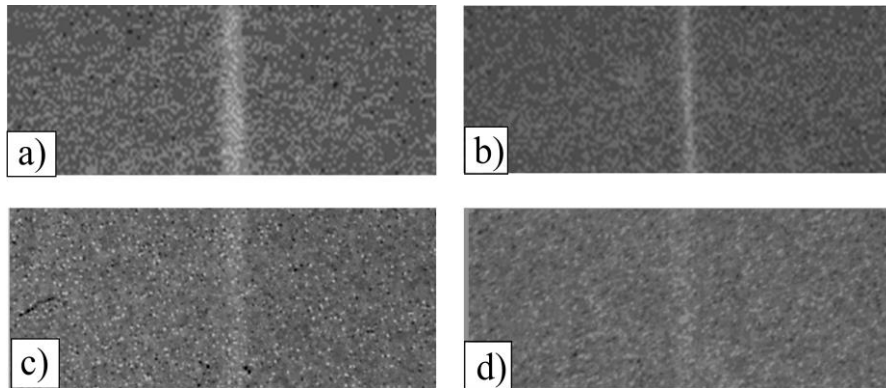


Figure 4. The foil images measured at the orientation of the Ta foil relative to the axis of radiation beam $\theta_f = 0,6^\circ$ and 0° , (a) and (b), respectively; (c) and (d) - at $\theta_f = 0,6^\circ$ and with the steel plate-absorbers 20 and 55 mm thick, respectively. The images enlarged additionally for demonstration.

Figure 5(a, d) shows the densitograms (normalized on their maxima) of the Ta foil images, which are shown in Figure 3(a, d). Densitograms were measured along lines that are perpendicular to the foil images. Densitograms show that at an angle $\theta_f = 0.6^\circ$, the width ΔL of the foil image at half height of densitogram increases by 1.4 times, but with additional steel plates, (c) and (d), the width ΔL of the image does not change and is equal to 0.115 mm, as in the absence of the steel plate (a).

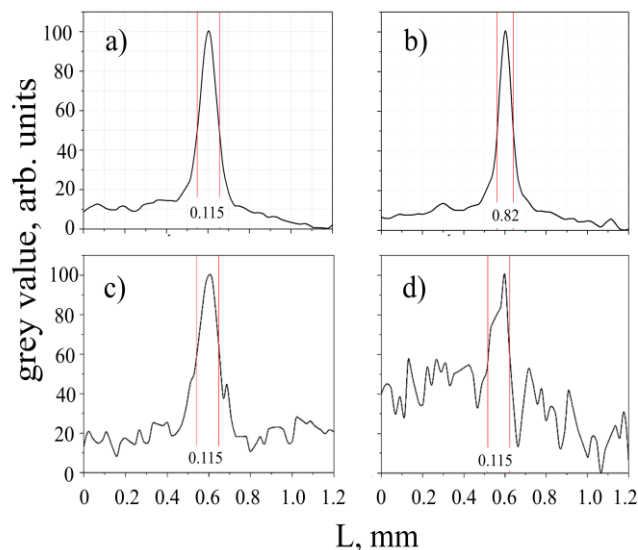


Figure 5. Densitograms of Ta foil images shown in Figure 4; (a) and (b) – the foil orientations $\theta_f = 0,6^\circ$ and 0° , respectively; (c) and (d) – at $\theta_f = 0,6^\circ$ and with the steel plate-absorbers 20 and 55 mm thick, respectively.

The width of the foil image can be estimated as $S_f = L_2((t_f + l_f \theta_f) + t_e) / L_1 - t_e$, where $t_f = 13 \mu\text{m}$ and $l_f = 4 \text{ mm}$ are the thickness and length of the Ta foil, $L_1 = 48 \text{ cm}$ and $L_2 = 114 \text{ cm}$ are the distances from the Ta target to the Ta foil and to the X-ray film, t_e is the thickness of the Ta target and θ is the angle of inclination of the Ta foil relative to the direction of radiation. The value of the width of foil image increases linearly with increasing the angle θ . For example, $S_f = 0.148 \text{ mm}$ at $\theta = 0.6^\circ$, which is consistent with the width of the densitogram (a) at the grey value of 30 %.

5. Conclusion

The presented experimental results show that it is possible to successfully use microfocus hard Bremsstrahlung generated in a narrow internal target of 18 MeV betatron, whose width is about 115

times smaller than the diameter of the electron beam, to obtain magnified images of microdefects in products made of heavy materials with high resolution.

The magnified images of the sample consisted of four steel blocks demonstrated a high resolution of three 10 μm gaps between adjacent blocks due to the small horizontal size of the linear focus of the Bremsstrahlung source. The magnified images of 13 μm Ta foil oriented at small angles relative to the radiation direction demonstrated its high resolution due to the small horizontal size of the linear focus of Bremsstrahlung source too. The image is more pronounced when the projection of the Ta foil is comparable to the size of the radiation focus. The images obtained at different thicknesses of the steel plate-absorber of the soft part of the radiation spectrum placed behind the Ta foil, which also simulates the Ta inclusion in the steel thickness, showed that such a defect can be detected at the steel thicknesses more than 55 mm.

It should be noted that microfocus tubes widely used for various purposes have reached the photon energy of Bremsstrahlung radiation of 750 keV, which allows radiography of the structure of steel samples with a thickness of not more than 60 mm [6]. The betatron generates microfocus radiation with a spectrum up to the electron energy. Therefore, a betatron-based microfocus source can be used for inspection of thicker samples.

The results indicate the high quality of the radiation beam generated by a microfocus source based on a compact betatron, which can also be used in laboratory physics experiments, for example, in materials science to study the internal boundaries of the media and microdefects in the composite materials or to study the effects of gamma optics.

Acknowledgments

This work is supported by the Russian Science Foundation, the project No. 17-19-01217.

References

- [1] Rychkov M M, Kaplin V V, Sukharnikov K and Vaskovskii I K 2016 Generation of X-ray radiation at the grazing incidence of 18 MeV electrons on a thin Si crystal in a betatron chamber *JETP Lett* **103**(11) 723
- [2] Pushin V S and Chakhlov V L 1997 *Patent RU* 2072643 <http://www.findpatent.ru/patent/207/2072643.html>
- [3] Yamada H 2003 Novel X-ray source based on a tabletop synchrotron and its unique features *Nucl. Instrum. Meth. B* **199** 509 http://www.cituk-online.com/acatalog/Section_NDT_Digital_Radiography_Calibration_Devices.html
- [5] Wilkins S V, Gureyev T E, Gao D, Pogany A and Stevenson A W 1996 Phase-contrast imaging using polychromatic hard X-rays *Nature* **384** 335
- [6] The Nikon Metrology X-ray Products: <http://x-sight.co.za/products/54/750-kv-microfocus-x-ray-source/>